Pushing the limits of SPM

by Joost W. M. Frenken[†]*, Tjerk H. Oosterkamp[†], Bas L. M. Hendriksen[†], and Marcel J. Rost[†,‡]

In the two decades since the invention of the scanning tunneling microscope (STM)[1], the family of local probing techniques known as scanning probe microscopy (SPM) has come to full maturity. Nowadays, the quality with which nanoscale images can be obtained and local spectroscopic information acquired using these instruments is spectacular. In addition, the ease of use of these machines has improved so much that they have found their way into the laboratories, not just of physicists, but also chemists, biologists, and engineers.

STMs, atomic force microscopes (AFMs), and other types of SPM instrumentation can be purchased off the shelf from several commercial companies for a wide variety of applications. This article reviews two recent developments in SPM technology: high-speed imaging and imaging under extreme conditions. Both developments illustrate how this technology is continuing to expand and enter new scientific and technological territory.

Breaking the speed limit

One of the serious, inherent limitations in all forms of SPM is the low imaging rate. This is because each image is built up pixel by pixel in a sequential scan of the surface. The scanning motion involves electronically controlled mechanical displacements, and usually some form of feedback is applied between a control parameter, such as tunneling current or force, and the height of the probe, e.g. the tip. Each of these elements introduces its own characteristic time restrictions, and together they conspire to make the acquisition time of STM, AFM, and other SPM images lengthy – typically between several seconds and several minutes per image.

Faster scanning would bring several distinct advantages. The most obvious of these is the possibility of following dynamic processes in real time[2-4]. There are already numerous examples of SPM studies on surface dynamics in which a series of images is recorded to generate a movie of the dynamic process[5]. For example, Fig. 1 shows three images taken from an STM movie on a Cu(001) surface in which four embedded In atoms are followed in their motion

[†]Kamerlingh Onnes Laboratory, Leiden University, and

[‡]Leiden Probe Microscopy, B.V.

P.O. Box 9504,
2300 RA Leiden, The Netherlands
*E-mail frenken@physics.leidenuniv.nl

ISSN:1369 7021

through the Cu surface[6-10]. From a quantitative analysis of the displacement statistics, this motion is shown to be solely the result of the presence of a low density of highly mobile surface vacancies in the Cu surface – an effect nicknamed the 'atomic slide puzzle'. Elsewhere in this issue, Besenbacher *et al.*[11] discuss STM movies in which oxygen molecules and oxygen vacancies are followed in detail during their diffusion on a TiO_2 surface[12]. Other examples of dynamic surface phenomena investigated by SPM imaging are heterogeneous catalysis (see below), crystallization of polycrystalline thin films[13], crystal growth[14-16], dynamics of DNA protein complexes[17], and conformational changes of membrane proteins[18]. When the imaging rate is low with respect to these processes, the images are blurred and the information about the dynamics is lost. The traditional approach is then to set the conditions of, for example, temperature or supersaturation to slow down the process and make it match the slow imaging rate in the hope that the physics of the process remains unchanged.

A second advantage of high-speed scanning is the generation of a much larger number of images or other form of scanning probe data in the same acquisition time. This greatly improves the statistics of the numerical information extracted from the images, e.g. atom, vacancy, cluster, island, or step densities, correlation functions, probability distributions of diffusion events, etc.

In a broader perspective, perhaps the greatest added value of high-speed data acquisition is that it will introduce the natural 'touch and feel' of, say, a hand-held video camera into SPM imaging. Imagine, for example, being able to turn some knobs or manipulate a joystick and have the complete SPM image respond instantly, e.g. by panning (shifting) or rotating the view; zooming in or out; or changing the 'contrast' via feedback controls such as the setpoint, gain, and filter settings. This will make the instrument not just faster to use but easier too. With high-speed imaging, finding an area or feature of interest and optimizing the image quality will require significantly less experience (and patience!) than is customary now.

We are working on both the mechanical and electronics aspects that need to be addressed in order to speed up SPM technology[19]. With STM imaging, we have achieved true video rate and faster[20], i.e. rates of at least 25 images/s, with a 'mature' image size of 256 x 256 pixels. Faster movies are possible when the number of pixels is reduced and vice versa.

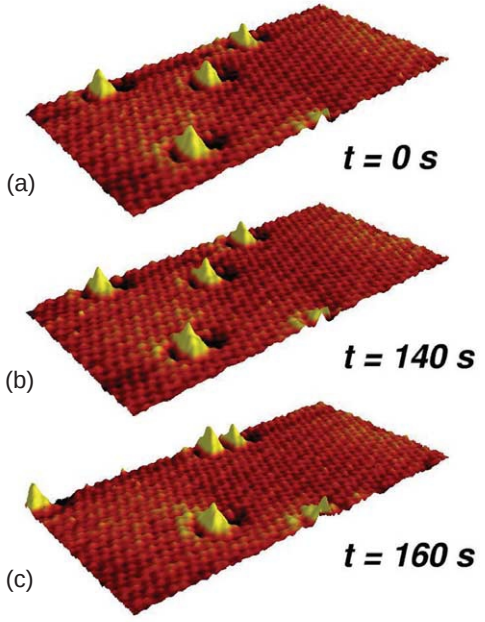

Fig. 1 Illustration of the power of SPM movies[5]. Three atomically resolved STM images (14 x 7 nm²) show the diffusion of four embedded In atoms within the outermost layer of a Cu(001) surface. During the first 140 s, the atoms are stationary, while in the next time interval of 20 s all four move over multiple lattice spacings. This peculiar motion is because of 'slide-puzzle' diffusion of surface vacancies in the Cu lattice[6-10]. (Reprinted with permission from[6]. © 2000 Nature Publishing Group.)

Let us briefly consider some of the essential elements of the electronics for the specific example of STM imaging[21]. In order to image surfaces with full atomic resolution even at the high pixel rates discussed here, the entire system should operate at a bandwidth of roughly 600 kHz, which is unusually high for SPM technology. Of course, a high bandwidth is accompanied by a high noise level. Therefore, maximum attention must be given to the signal-to-noise ratio of all components in the system. The additional bonus of such an exercise is that the optimized high-speed control system will also have a superb, i.e. low-noise, performance when used at low bandwidths.

Fig. 2 shows a diagram of the electronics we use for high-speed STM imaging. One of the most difficult components is the preamplifier, which acts as a current-to-voltage converter. We have developed several high-frequency preamplifiers based on field-effect transistors and equipped with appropriate compensation networks. With these, we operate at 1 V/nA conversion with a noise output corresponding to 0.1 nA r.m.s. input noise integrated over the full 600 kHz bandwidth.

Another special feature of our electronics (Fig. 2) is that we not only record the height control signal *z*, which is fed

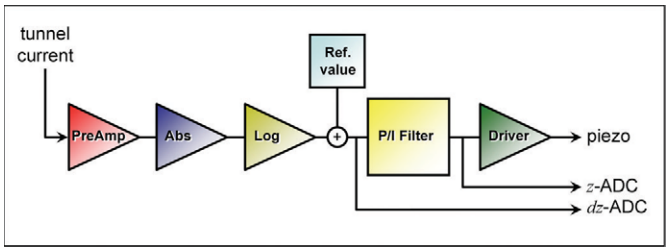

Fig. 2 Schematic of the feedback circuit used for high-speed STM imaging[21]. The preamplifier (PreAmp) converts the tunneling current into a voltage. The next two elements (Abs and Log) produce the logarithm of the absolute value of this voltage, which serves as a measure for the tip-surface distance. At the summing point, this signal is compared with a reference value to obtain the deviation dz between the actual tip height and the optimal height. This error signal is used as input for the filter (P/I), which combines adjustable amounts of proportional amplification and integration to generate the control signal z for the piezo element. The high-voltage amplifier (Driver) brings this control signal into the typical -200 V to +200 V range required for the piezo elements in STMs. Both the height signal z and the residual error dz are recorded by separate analog-to-digital converters (ADCs) (after[20]).

back to the *z*-electrode of the STM piezo element, but also the residual error signal *dz*[20,22]. This error corresponds to high-frequency variations in the tunneling current, starting at frequencies just below the mechanical eigenfrequencies of the scanner. Recording both *z* and *dz*, we can allow *z* to be sufficiently strongly low-pass filtered to keep the STM feedback system from spontaneously resonating without losing any information at higher frequencies (Fig. 3). In other words, we allow our STM to scan in a 'hybrid' mode between the traditional modes of constant-current imaging and constant-height imaging. By recording the low-frequency height control signal *z* and the residual error signal *dz*, we can reconstruct the 'ideal' surface contour $z + dz$ that the tip would have followed at low scan speeds. Fig. 4 demonstrates this image reconstruction for a Cu(001) surface with several monatomic steps in the field of view[20]. Even though the scan speed here is modest, the uncorrected height image shows significant rounding of the steps and, correspondingly, the steps stand out strongly in the error image.

In addition to optimization of the electronics, the mechanical part of the STM also requires special attention. Most SPM instruments have mechanical resonances at frequencies as low as a few kilohertz. Even when the feedback system is filtered well enough not to excite these resonances (see above), the rapid *x,y*-scanning motion can be too 'violent' for such mechanical structures. A partial remedy is to abandon traditional linear scanning, which introduces a strong acceleration at the turning point at the end of each scan line, and replace this with either a rounded triangular wave form or even a sine wave[23]. For our high-speed applications, we find it essential to combine such smoothed scanning motion with a much stiffer mechanical design of the scanner. For this purpose, the housing is typically made to be heavy and rigid, while the piezo element is kept as light and rigid as possible. For example, Fig. 5 shows an STM image obtained in air on a graphite surface. It is a single frame taken from a movie that we recorded at an image rate of 80 Hz. For this measurement, we used a tiny piezo stack with two shear-mode piezos for the *x* and *y* motion, and one regular piezo plate for motion in the *z* direction. The lowest mechanical resonance frequency of this piezo-stack scanner is as high as 64 kHz, and is sufficient to avoid resonance problems at the 10 kHz line rate of Fig. 5.

We are working on alternative architectures that combine high resonance frequencies with large scan ranges. A very

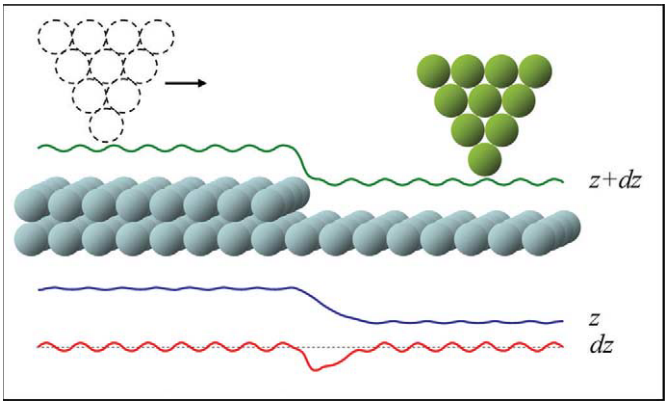

Fig. 3 The combination of the actual path z followed by the STM tip at high speeds and the high-frequency residual error signal dz is used to reconstruct the 'ideal' trajectory z + dz that the tip would follow at low speed.

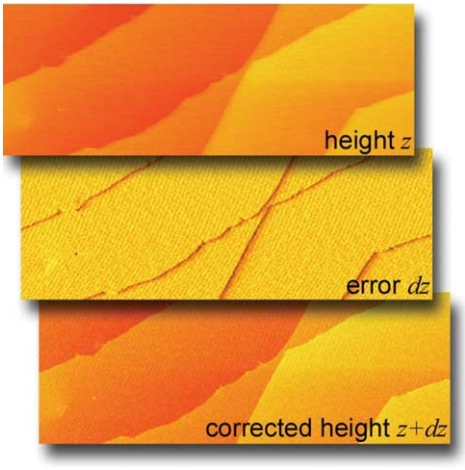

Fig. 4 Reconstruction of the corrected or 'ideal' image z + dz from the height z and residual error signal dz for a Cu(001) surface; 83 x 31 nm² selections from 200 x 200 nm² STM images (after[20]).

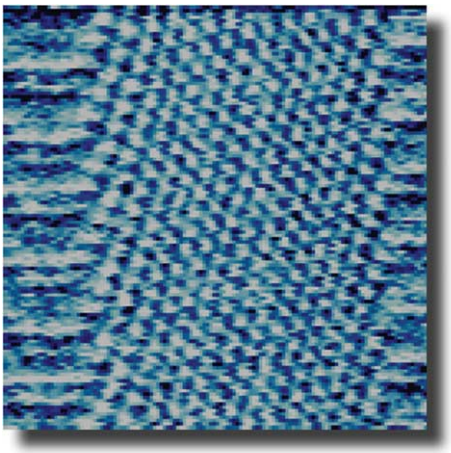

Fig. 5 Snapshot from a high-speed STM movie. The image (128 x 128 pixels) shows the atomic lattice of a graphite surface scanned in air with a PtIr tip (raw data). The STM movie was recorded at a frame rate of 80 images/s. The characteristic distortions at the left and right sides of this image reflect the smooth acceleration and deceleration at the beginning and end of each scan line, which is necessary to avoid excitation of mechanical resonances of the scanner. These distortions can be corrected for easily, but they are shown here for clarity. Note that the image only contains the scan lines in which the tip moved from left to right. A similar image (size and quality) can be composed (not shown) from all intermediate lines in which the tip ran back from right to left (after[20]).

promising, novel geometry in this respect is that of a conical piezo element, which has higher lateral stiffness and lower effective mass than the piezo tubes used traditionally[24].

Harsh conditions

The examples of high-speed imaging of dynamic surface processes presented above could be perceived as being rather academic, as they involve well-defined, single-crystal surfaces under highly idealized conditions such as ultrahigh vacuum. However, one of the enormous strengths of SPM techniques is that many of them should, at least in principle, continue to operate under harsh conditions. STMs, AFMs, and other SPM tools do not suffer from the problems that most particle (atom, molecule, ion, or electron)-based techniques do when their vacuum is to be replaced by a gas atmosphere or liquid. This makes SPMs ideal tools to investigate a wide range of microscopic aspects of processes with direct relevance to applications. For example, STMs can be used with the tip and sample immersed in electrolytic solutions to follow electrochemical processes on the atomic scale[25,26]. AFMs are used inside liquids to follow the growth of protein crystals from mildly supersaturated solutions[14-16]. Similarly, AFM techniques can investigate molecular processes in living organisms, e.g. on biological membranes and cell walls[27].

Here, we focus on the development of an STM for the 'live' observation of catalysis, or rather, of the catalyst surface while it is at work under semirealistic conditions: high pressures of appropriate gas mixtures and high temperatures. Clearly, this is an area of great practical relevance, since hardly any technique is capable of probing the atomic-scale details of surfaces under the high-pressure, high-temperature conditions required in practical catalysis. This means that much of our current atomic-scale understanding of heterogeneous catalysis is based on low-pressure, low-temperature observations obtained with a variety of microscopy and spectroscopy techniques in ultrahigh-vacuum chambers[28]. The ten orders of magnitude that separate the low pressures used in these observations from the typical pressures of practical catalysis are usually referred to as the 'pressure gap'. There are several approaches that one can take to cross this gap with the STM. The most straightforward of these is to mount an ultrahigh-vacuum-type STM in a vacuum chamber that can also be backfilled with the high-pressure gas mixture. Examples of this high-pressure-chamber approach can be found elsewhere[29-31]. A big advantage of this approach is that no concessions are necessary concerning imaging quality; even at high pressures, atomic resolution can be reached. However, there are also distinct disadvantages. Measuring the chemical reactivity, e.g. by mass spectrometry of the gas in the chamber, is necessarily insensitive because of the large ratio between the gas volume and the active surface area of the small sample. A more severe problem is that it is difficult to work at high sample temperatures. When the sample is hot, the heat transport through the gas makes it difficult to keep the essential STM components cool. Even more problematic are the convective flow patterns that result. Typically, these vary on a timescale of seconds, causing all temperatures in the STM to vary weakly on that timescale. This leads to variable expansions in the instrument and strong, erratic image distortions. Probably as a result of such problems, high-pressure studies in backfilled vacuum chambers have been conducted mainly at room temperature.

In order to make it possible to obtain STM images at high pressures *and* high temperatures, as well as combine STM imaging with fast reactivity monitoring, we have taken a different approach, illustrated in Fig. 6. Our STM is integrated with a small flow reactor cell, residing inside an ultrahigh-vacuum chamber[32,33]. After standard cleaning procedures in ultrahigh vacuum, the sample is pressed firmly against the open side of the cell, thereby sealing off the 500 µl volume of the cell from the surrounding vacuum. The inner surfaces of

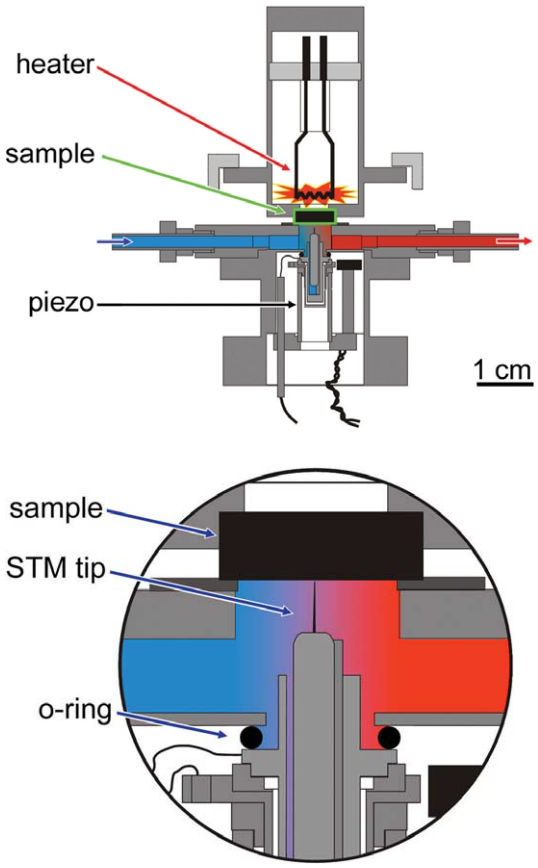

Fig. 6 Schematic cross section of the 'Reactor-STM'. The instrument can image a material surface while it is active as a catalyst under gas flow conditions at pressures up to 5 bar and temperatures up to 500 K. Apart from the surface of the sample, only the tip of the STM is in contact with the flowing, hot, high-pressure gas mixture. The inset shows how the scanning motion, generated by the external piezo element, is transferred to the STM tip inside the reactor cell via a flexible Viton O-ring. The volume of the cell is 500 µl. The gas enters the cell from the left (blue) and flows out on the right (red) after having been in contact with the sample. When the sample and its holder with integrated heater are pulled up, both the sample surface and the interior of the reactor are exposed to the ultrahigh vacuum of the surrounding setup, which further provides standard tools for preparation and characterization of clean, well-ordered metal surfaces (after[32,33]).

the invar cell are fully coated with a Au film so that (for most reactions) the only potentially active surface is that of the sample. Only the tip and a tiny tip holder of the STM are inside the reactor cell. The piezo tube that is responsible for the scanning motion of the tip is outside. A Viton® O-ring is used to seal the high-pressure cell from the vacuum around the piezo element. The flexibility of this ring is sufficient to allow the scanning motion to be transferred unhindered to the tip. Two Au gas lines run to the reactor. The first connects the reactor to a gas system that can control the composition, pressure, and flow rate of the gas mixture independently. The second serves as the exhaust and can be used to have a well-defined fraction of the reacted gas mixture leak into the ultrahigh-vacuum chamber, where its composition is analyzed by a quadrupole mass spectrometer. Because of the small volume of the reactor, the time resolution with which the gas is analyzed is just a few seconds, making it possible to correlate the reactivity with the structure observed by the STM on this short timescale.

In Fig. 7, we show example STM images obtained with this 'Reactor-STM' on a working catalyst under two slightly different operation conditions[5,34], both at 425 K and a total pressure of 0.5 bar. Here, a Pt(110) surface was used in the catalytic oxidation of carbon monoxide: $2CO + O_2 \rightarrow 2CO_2$. This reaction system has been studied extensively at low pressures with more or less the full spectrum of ultrahigh-vacuum-based surface science techniques. Our observations have revealed that a phase transition can occur at high pressures between two different surface structures. One corresponds to a well-ordered, flat Pt surface covered by a dense layer of CO molecules (Fig. 7, left panel). At higher P_{O_2}/P_{CO} ratios, an ultrathin, well-ordered surface oxide forms, which becomes rough over the course of time (Fig. 7, right panel). From our simultaneous measurements of the partial pressures of CO, O_2, and CO_2 in the reactor cell, we have learned that both structures are catalytically active but the conversion rates and reaction mechanisms are quite different. Where the structure on the left in Fig. 7 makes CO react with adsorbed O atoms – the Langmuir-Hinshelwood mechanism[28] – the oxide structure on the right of Fig. 7 should be regarded as an intermediate product rather than an alternative catalyst. In a Mars-van-Krevelen reaction, the CO molecules extract O atoms directly from the oxide layer, after which oxygen molecules quickly repair the damage to the oxide. Switching between the two structures is an abrupt, first-order

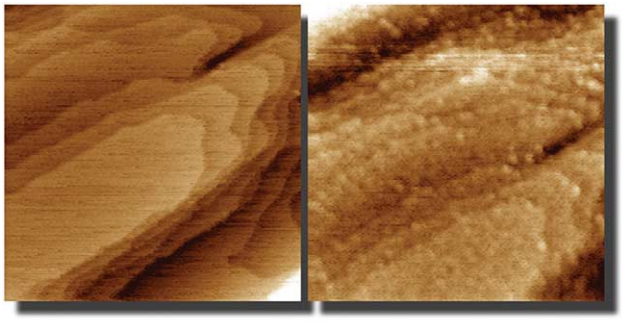

Fig. 7 Two STM images (210 x 210 nm^2) selected from an STM movie[5] obtained with the Reactor-STM of a Pt(110) surface in a 3.0 ml/min flow of a mixture of O_2 and CO at 425 K and a total pressure of 0.5 bar. The left image corresponds to an unreconstructed metallic Pt surface covered by a dense monolayer of CO molecules. The right image, obtained at a slightly higher partial pressure of O_2, shows a surface oxide that has become rough because of the reaction with CO (after[34]).

phase transition that takes place within a single STM scan line, i.e. well within 1 s. Furthermore, the mass spectra change abruptly within the 2 s time resolution of the spectrometer, which implies that the entire surface switches collectively. The partial pressure of CO_2, i.e. the reaction rate, jumps up by about a factor of three when the oxide forms.

Together with *ex situ* STM studies[35], these high-pressure observations have shed new light on surface oxides. It had been anticipated long before that oxides could form, e.g.[36], but the notion that they lead to high reactivity rather than act as a poison for the reaction is new. Additionally, the Mars-van-Krevelen mechanism is new in the context of CO oxidation. We have observed the same high-pressure, high-temperature phase transition from a metallic surface to a surface oxide accompanied by a clear improvement in reactivity for several low-index and stepped surfaces of Pt and Pd[37,38], indicating that this behavior is general for this class of systems. In addition to STM work, we have recently performed surface X-ray diffraction measurements on these surfaces. These have allowed us to resolve the detailed structure of the surface oxides formed[39]. Density functional theory calculations are also providing further insight[40].

Outlook

The two technical developments described in this article serve as examples of what is in store for SPM technology in the near future. On the one hand, SPMs will become faster and easier to use. They will provide a much more natural interface to the user, who will be able to operate them as if they were 'regular' video cameras fitted with 'nanovision'. On the other hand, further specialization of SPMs will occur toward special-purpose instruments for specific tasks under specific conditions. Both types of advance will add spectacular value to SPM technology by themselves, and the combination of the two will eventually lead to a new generation of versatile, fast, *in situ* SPM instruments for online, atomic-scale investigation and monitoring of a wide variety of relevant processes. MT

Acknowledgments

We are indebted to the electronics and mechanical workshops at the Science Faculty of Leiden University for their strong, high-level technical support of the projects described in this article. We also gratefully acknowledge the technical staff at the FOM-Institute for Atomic and Molecular Physics in Amsterdam, the Netherlands, who were involved in both projects at an early stage. This work has been partly supported by the Stichting Technische Wetenschappen (STW), the Stichting voor Fundamenteel Onderzoek der Materie (FOM), and the Nederlandse Organisatie voor Wetenschappelijk Onderzoek (NWO).

REFERENCES

1. Binnig, G., *et al., Phys. Rev. Lett.* (1982) **49** (1), 57
2. Kuipers, L., *et al., Phys. Rev. Lett.* (1993) **71** (21), 3517
3. Kuipers, L., *et al., Phys. Rev. B* (1995) **52** (15), 11 387
4. Hoogeman, M. S., *et al., Surf. Sci.* (2000) **447** (1-3), 25
5. www.physics.leidenuniv.nl/sections/cm/ip
6. van Gastel, R., *et al., Nature* (2000) **408**, 665
7. van Gastel, R., *et al., Phys. Rev. Lett.* (2001) **86** (8), 1562
8. Van Gastel, R., *et al., Surf. Sci.* (2002) **521** (1-2), 10
9. Somfai, E., *et al., Surf. Sci.* (2002) **521** (1-2), 26
10. van Gastel, R., *et al.*, Diffusion of vacancies in metal surfaces: theory and experiment, In *The Chemical Physics of Solid Surfaces*, Woodruff, D. P. (ed.), Elsevier, Amsterdam, (2003) **11**, 351
11. Besenbacher, F., *et al., Materials Today* (2005) **8** (5), 26
12. Schaub, R., *et al., Science* (2003) **299**, 377
13. Rost, M. J., *et al., Phys. Rev. Lett.* (2003) **91**, 026 101
14. Vekilov, P. G., *Prog. Cryst. Growth Charact. Mater.* (2002) **45** (3), 175
15. Chew, C. M., *et al., Cryst. Growth Des.* (2004) **4** (5) 1045
16. Land, T. A., and De Yoreo, J. J., *J. Cryst. Growth* (2000) **208** (1-4), 623
17. Kasas, S., *et al., Biochem.* (1997) **36** (3), 461
18. Engel, A., and Müller, D. J., *Nat. Struct. Biol.* (2000) **7** (9), 715
19. Kuipers, L., *et al., Rev. Sci. Instrum.* (1995) **66** (9), 4557
20. Rost, M. J., *et al., Rev. Sci. Instrum.*, accepted
21. For a description of standard STM electronics, see e.g. Chen, C. J., *Introduction to Scanning Tunneling Microscopy*, Oxford University Press, New York, (1993)
22. Hosaka, S., *et al., Rev. Sci. Instrum.* (1990) **61** (4), 1342
23. Wintterlin, J., *et al., Surf. Sci.* (1997) **394** (1-3), 159
24. Frenken, J. W. M., and Van Loo, W., Dutch Patent Application 1026929, (2004)
25. Broekman, P., *et al., Surf. Rev. Lett.* (1999) **6** (5), 907
26. Dieluweit, S., and Giesen, M., *J. Electroanal. Chem.* (2002) **524-525**, 194
27. You, H. X., and Yu, L., *Methods Cell Sci.* (1999) **21** (1), 1
28. Somorjai, G. A., *Introduction to surface chemistry and catalysis*, John Wiley & Sons, New York, (1994)
29. McIntyre, B. J., *et al., Rev. Sci. Instrum.* (1993) **64** (3), 687
30. Jensen, J. A., *et al., J. Vac. Sci. Technol. B* (1999) **17** (3), 1080
31. Laegsgaard, E., *et al., Rev. Sci. Instrum.* (2001) **72** (9), 3537
32. Hendriksen, B. L. M., Model Catalysts in Action, High-Pressure Scanning Tunneling Microscopy, PhD thesis, Leiden University, The Netherlands (2003)
33. An early version of the Reactor-STM has been described in Rasmussen, P. B., *et al., Rev. Sci., Instrum.* (1998) **69** (11), 3879
34. Hendriksen, B. L. M., and Frenken, J. W. M., *Phys. Rev. Lett.* (2002) **89**, 046 101
35. Over, H., *et al., Science* (2000) **287**, 1474
36. Turner, J. E., *et al., Surf. Sci.* (1981) **109** (3), 591
37. Hendriksen, B. L. M., *et al., Surf. Sci.* (2004) **552** (1-3), 229
38. Hendriksen, B. L. M., and Frenken, J.W.M., *Catal. Today*, to be published
39. Ackermann, M. D., *et al.*, in preparation
40. Reuter, K., *et al., Phys. Rev. Lett.* (2004) **93** (11), 116 105